

Femtosecond laser fabrication of high reflectivity micromirrors

D. Brodoceanu,¹ G. D. Cole,² N. Kiesel,² M. Aspelmeyer,² and D. Bäuerle^{1,a)}

¹Institute for Applied Physics, Johannes-Kepler-University Linz, Altenbergerstr. 69, A-4040 Linz, Austria

²Faculty of Physics, University of Vienna, Boltzmannngasse 5, A-1090 Vienna, Austria and Institute for Quantum Optics and Quantum Information (IQOQI), Austrian Academy of Sciences, Boltzmannngasse 3, A-1090 Vienna, Austria

(Received 7 April 2010; accepted 2 July 2010; published online 26 July 2010)

High-quality freestanding micromirrors consisting of 40 dielectric layers on silicon have been fabricated by ultrashort-pulse laser ablation in combination with laser-assisted wet chemical etching. Backside material removal enables direct access to both faces of the dielectric coating. The amplitude reflectance of the micromirrors has been determined by Fabry–Pérot interferometry; a finesse in excess of 8900 ± 700 , corresponding to a reflectivity exceeding 99.95%, has been found. The mechanical quality factor, Q , of the microresonators, measured at 20 K, is determined to be between 5000 and 6000. © 2010 American Institute of Physics. [doi:10.1063/1.3467846]

Microelectromechanical systems (MEMS) continue to gain increasing importance in numerous areas of modern technology. Rapid advancements in fabrication processes permit mass production of sensors with minimum size, weight, and power consumption that are tailored for a wide variety of applications.^{1–3} The operating principle of MEMS relies on the mechanical motion of micromachined components such as cantilevers, suspended bridges, etc. The changes in mechanical properties of these components relating to physical, chemical, or biological stimuli can be measured, for example, by means of electronic or optical coupling. The variation in resonance frequency (or additionally in phase or displacement amplitude) of microresonator-based devices, provides information about the interactions between the sensor and its environment.

With optical read-out schemes, Fabry–Pérot interferometers are commonly used. The sensitivity of such systems is strongly dependent on the reflectivity of the resonator, as well as on its mechanical quality factor.⁴ Beyond classical sensing applications, efforts to observe quantum mechanical effects with micromirror oscillators^{5–9} are currently limited by thermal noise, arising from the dynamic equilibrium between the mechanical energy of the device and the thermal energy of the surrounding environment. Thus, poor mechanical quality factor limits the performance of devices operating in resonance mode. The fabrication of high mechanical quality resonators with ultrahigh reflectivity is a prerequisite for enhancing the performance of such devices.

In this letter, we describe the fabrication of high-reflectivity and high mechanical quality factor microresonators, consisting of a suspended stack of dielectric layers comprising a multilayer distributed Bragg reflector (DBR). For the construction of these devices we use a combination of ultrashort-pulse laser ablation and laser-assisted wet etching.^{10,11} These techniques can be applied to a wide variety of materials and offer precise process control, enabling the realization of high performance optomechanical resonators.

One of the preferred materials for microsystems development is single-crystal silicon. In the present investigation

we utilize small chips cut from a 4 in. (100) Si wafer with a high-reflectivity coating consisting of 40 alternating layers of quarter-wave Ta_2O_5 and SiO_2 (high reflectivity stopband centered at 1064 nm). The multilayer was prepared by ion beam sputtering (IBS) at a commercial vendor (ATFilms, Boulder, CO, USA). The total thickness of the DBR is $5.4 \mu\text{m}$. Laser ablation is performed on the rear side of the silicon wafer by scanning a focused Ti:sapphire laser beam ($\lambda=800 \text{ nm}$, $\phi \approx 2.4 \text{ J}/\text{cm}^2$, and $\tau=1 \text{ ps}$) across a pre-defined area of $600 \times 1500 \mu\text{m}^2$ until the thickness of the silicon is reduced from the original nominal value of $500 \mu\text{m}$ to approximately $50 \mu\text{m}$ [Fig. 1(a)]. A stream of air is used to avoid redeposition of debris during ablation. Subsequently, the remaining silicon is removed by laser-assisted wet etching ($\lambda=800 \text{ nm}$, $\phi \approx 25 \text{ mJ}/\text{cm}^2$, and $\tau_\ell=5 \text{ ps}$) in 40% aqueous NaOH solution until the high reflectivity Bragg mirror is left free standing. During the ablation and etching processes, the dielectric coating is protected by a thin layer of photoresist. Definition of the microresonators is performed by laser ablation of the free-standing DBR from the backside of the sample [Fig. 1(b)]. Here, frequency doubled 400 nm Ti:sapphire laser pulses ($\phi \approx 1.8 \text{ J}/\text{cm}^2$ and $\tau_\ell=200 \text{ fs}$) are employed. Focusing is performed by means of a cylindrical lens ($f=8 \text{ mm}$). By this means the DBR is shaped into smooth and well-defined microresonators as shown in Fig. 2.

Ultrashort-pulse laser ablation permits controlled micro-fabrication with little or no thermal damage to the surround-

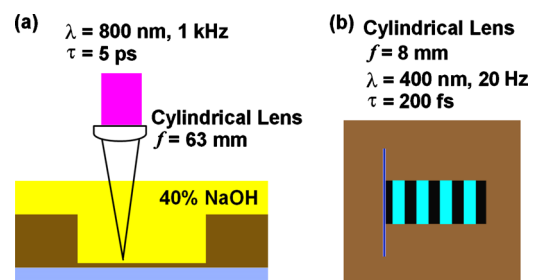


FIG. 1. (Color online) Main steps involved in the fabrication of microresonators. (a) Cross-section of the structure showing laser-assisted etching of the remaining Si after laser ablation. (b) Patterning of the microresonators by ablation of the free standing membrane using a line focus with a cylindrical lens (ablated regions in black).

^{a)}Electronic mail: dieter.baeuerle@jku.at.

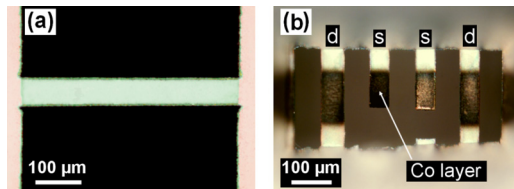


FIG. 2. (Color online) Optical micrographs of the microresonators. (a) Front view; (b) image taken from the rear side of the sample showing singly (s) clamped and doubly (d) clamped microresonators coated with 200 nm Co.

ing material.¹⁰ With the laser pulse lengths under consideration, the width of the heat affected zone (HAZ) can be estimated from the simple expression $\ell_T \approx 2\sqrt{D\tau_\ell}$, where ℓ_T is the heat diffusion length, D the thermal diffusivity of the material, and τ_ℓ the laser pulse duration. Using Si and 1 ps pulses, we find $\ell_T \approx 10$ nm, verifying the small spatial extent of the HAZ.

Laser-assisted dry- or wet-etching has been demonstrated to be a viable technique for “gentle” three-dimensional patterning of materials, including those that cannot be patterned efficiently by other techniques. Depending on the material, the etchant, and the laser parameters, the microscopic mechanisms involved in the process can be purely photochemical (nonthermal), purely photothermal, or a combination of the two (photophysical). With the system under consideration and the laser parameters employed, etching of Si is mainly thermal and based on local heating.¹⁰ Within the kinetically controlled regime, the reaction rate depends exponentially on temperature. The temperature dependence of the thermal conductivity of Si can be approximated by $\kappa(T) \approx \kappa(T_0)/T^{*n}$ where $T^* \equiv T/T_0$. Here, T_0 is the temperature outside of the laser processed region and $n(\text{Si}) \approx 1.22$.¹⁰ Thus, by applying the Kirchhoff transform, we find that the laser-induced temperature rise depends nonlinearly on laser fluence. This double nonlinear behavior results in a strong localization of the etching process. In liquid-phase processing using ultrashort laser pulses, the high peak temperatures result in the formation of microbubbles at the liquid-solid interface due to local boiling of the liquid. The formation of bubbles and, occasionally, their coalesce, cause a decrease in transport rates and thereby diminishes the overall etch rate. To suppress this process and ensure uniform etching, the NaOH solution is recirculated with a peristaltic pump. To avoid substrate ablation, etching was performed with lower fluences and longer pulses ($\lambda=800$ nm, $\phi \approx 25$ mJ/cm², and $\tau_\ell=5$ ps). Under these conditions, the etch rate is estimated to be about 0.02 Å/pulse (2 nm/s at 1 kHz repetition rate). The SiO₂ layer from the base of the DBR acts as an effective etch stop due to its very low etch rate in the NaOH solution. Thus, etching is self-terminating once all traces of the silicon are removed.

The precise shaping of the fragile microresonators demonstrates another advantage of laser micromachining: almost no mechanical forces are involved in this process. With the present material, ultrashort laser pulses permit damage-free high aspect-ratio etching/ablation of the DBR (Fig. 2). The design further permits the deposition of additional layers of various materials for functionalization onto the rear side of the micromirror. As an example, for driving the mechanical oscillation of the resonator by means of an external magnetic field, a 200 nm thick cobalt layer has been deposited on the

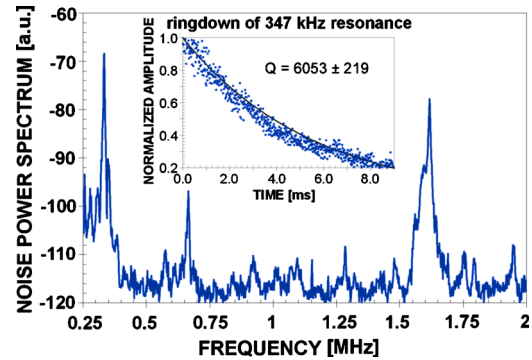


FIG. 3. (Color online) Cryogenic (20 K) frequency response of a doubly clamped $220 \times 50 \mu\text{m}^2$ Co coated microresonator driven with wide-band white noise from a high frequency piezo disk in vacuum. The inset displays the free ringdown of the fundamental mode as used for quality factor determination.

rear side of the cantilevers via thermal evaporation [Fig. 2(b)]. Both singly clamped and doubly clamped microresonators with widths of 40 to 80 μm , and lengths between 90 and 450 μm are fabricated using the procedure outlined above. Based on these dimensions, the total mass of the microresonators is estimated to be between 120–1050 ng.

The optical properties of the devices are characterized by Fabry–Pérot interferometry. In this experiment, the wafer is mounted on a three-axis translation stage with the micromirror facing a massive concave mirror, forming the resonant cavity. Optical interrogation of this cavity is realized through careful alignment to a free-space 1064 nm Nd:YAG laser source.

With an input coupler reflectivity of 99.970%, we record a finesse of 8900 ± 700 for the samples. This corresponds to an amplitude reflectance of $99.958\% \pm 0.006$ at 1064 nm for the postprocessed devices. For comparison, the nominal reflectivity of the unprocessed Bragg coating is 99.967%. This result proves that the quality of the high reflecting mirror is preserved during the fabrication process.

The mechanical quality factor, Q , is an important parameter for assessing the performance of resonant MEMS sensors. A high mechanical quality factor represents a low energy loss in each period of vibration. Here, Q is measured via free ringdown of the resonator. The device is driven on resonance with a sinusoidal input (devices are excited via inertial drive with a high frequency piezo disk mounted beneath the chip); once the equilibrium amplitude is reached, the drive signal is shut off and the exponential decay of the ringing structure is recorded via homodyne interferometry with data capture enabled by a high-speed oscilloscope. Free-ringdown is performed in vacuum (10^{-7} mbar at 20 K) to avoid excess loss induced by fluidic damping. Furthermore, in order to investigate the temperature dependence of the mechanical Q , the sample is held in a continuous flow ⁴He cryostat, allowing for measurement from 300 to 4 K with proper radiation shielding.

Figure 3 shows the frequency response measured on a $220 \times 50 \mu\text{m}^2$ doubly clamped Co coated beam driven with wide-band white noise. The frequency of the fundamental mode is geometry dependent and ranges from a low of around 100 kHz to approximately 500 kHz. The quality factor determined in vacuum at room temperature using the free-ringdown technique is between 300 and 600 for both uncoated and Co coated microresonators, with damping im-

posed by thermoelastic effects.¹² Upon cooling to 20 K, the damping is reduced significantly and the Q increases to a relatively constant value between 5000 and 6000. At cryogenic temperatures the damping is dominated by internal materials losses, as previously investigated in the laser interferometer gravitational wave observatory campaign.¹³ We estimate that the phonon-tunneling limited quality factor¹⁴ (commonly referred to as anchor loss) for these devices exceeds 1×10^5 , (for example, a $220 \times 50 \mu\text{m}^2$ doubly clamped beam shows a theoretical Q value of 1.14×10^5).

Both the optical and mechanical properties of the low-mass micromirrors strongly depend on the material composition of the DBR. In comparison with other dielectric systems, previously investigated high reflectivity micro-oscillators fabricated from $\text{SiO}_2/\text{TiO}_2$ have yielded a Q factor of 9000. However, the achievable finesse in these devices was limited to ~ 500 , corresponding to a reflectivity of about 99.6%.⁹ By switching to the $\text{SiO}_2/\text{Ta}_2\text{O}_5$ multilayer structure as investigated in the present experiments enables a significant improvement in the optical properties of the Bragg mirror. The finesse in this case is nearly 9000, similar to that achieved with recent devices using the same $\text{SiO}_2/\text{Ta}_2\text{O}_5$ multilayer.^{15,16} The quality factor of our laser fabricated micromirrors is currently limited by the intrinsic material loss attributed to the high index Ta_2O_5 layers¹³ but still approaches the damping rate in state of the art systems.^{15,16} Further improvements in Q using a nearly identical structure may be realized by following similar routes as those explored in the gravitational wave community, with one possibility being the use of titania-doped coatings.¹⁷

In summary, we have demonstrated an efficient method for producing free-standing high reflectivity micromirrors using ultrashort-pulse laser ablation in combination with laser-assisted wet etching. The back side etch process enables the fabrication of microresonators with direct access to *both* faces of the DBR. This is an important step for experimental configurations in which two laser beams are simultaneously focused on the free standing DBR from opposite directions.¹⁸ Furthermore, this design permits the deposition of additional layers of various materials onto the rear side of the micromirror. The excellent control achieved with this fabrication technique demonstrates the advantages of femto-second laser microprocessing for the fabrication of high-performance optomechanical resonators.

We wish to thank the Austrian Research Fund FWF (Fonds zur Förderung der wissenschaftlichen Forschung) under Contract No. L426-N20 for financial support. G.D.C. is a recipient of a Marie Curie Fellowship of the European Commission and N.K. of a Feodor-Lynen research Fellowship from the Alexander von Humboldt Foundation.

¹N. V. Lavrik, M. J. Sepaniak, and P. G. Datskos, *Rev. Sci. Instrum.* **75**, 2229 (2004).

²J. J. Allen, *Micro Electro Mechanical System Design* (CRC, Boca Raton, 2005).

³H. Baltes, O. Brand, G. K. Fedder, and C. Hierold, *Enabling Technologies for MEMS and Nanodevices (Advanced Micro and Nanosystems)* (Wiley, Weinheim, 2004).

⁴D. Kleckner, W. Marshall, M. J. A. de Dood, K. N. Dinyari, B.-J. Pors, W. T. M. Irvine, and D. Bouwmeester, *Phys. Rev. Lett.* **96**, 173901 (2006).

⁵G. J. Milburn, K. Jacobs, and D. F. Walls, *Phys. Rev. A* **50**, 5256 (1994).

⁶M. D. LaHaye, O. Buu, B. Camarota, and K. Schwab, *Science* **304**, 74 (2004).

⁷M. Pinard, A. Dantan, D. Vitali, O. Arcizet, T. Briant, and A. Heidmann, *Europhys. Lett.* **72**, 747 (2005).

⁸S. Gigan, H. R. Böhm, M. Paternostro, F. Blaser, G. Langer, J. B. Hertzberg, K. C. Schwab, D. Bäuerle, M. Aspelmeyer, and A. Zeilinger, *Nature (London)* **444**, 67 (2006).

⁹H. R. Böhm, S. Gigan, F. Blaser, A. Zeilinger, M. Aspelmeyer, G. Langer, D. Bäuerle, J. B. Hertzberg, and K. C. Schwab, *Appl. Phys. Lett.* **89**, 223101 (2006).

¹⁰D. Bäuerle, *Laser Processing and Chemistry*, 3rd ed. (Springer, Berlin, Heidelberg, 2000).

¹¹*Laser Ablation and Desorption*, Experimental Methods in the Physical Science, edited by J. C. Miller and R. F. Haglund (Academic, London, 1998), Vol. 30.

¹²R. Lifshitz and M. L. Roukes, *Phys. Rev. B* **61**, 5600 (2000).

¹³S. D. Penn, P. H. Sneddon, H. Armandula, J. Betzwieser, G. Cagnoli, J. Camp, D. R. M. Crooks, M. M. Fejer, A. M. Gretarsson, G. M. Harry, J. Hough, S. E. Kittelberger, M. J. Mortonson, R. Route, S. Rowan, and C. C. Vassiliou, *Class. Quantum Grav.* **20**, 2917 (2003).

¹⁴I. Wilson-Rae, *Phys. Rev. B* **77**, 245418 (2008).

¹⁵S. Gröblacher, S. Gigan, H. R. Böhm, A. Zeilinger, and M. Aspelmeyer, *EPL* **81**, 54003 (2008).

¹⁶S. Gröblacher, J. B. Hertzberg, M. R. Vanner, G. D. Cole, S. Gigan, K. C. Schwab, and M. Aspelmeyer, *Nat. Phys.* **5**, 485 (2009).

¹⁷G. M. Harry, M. R. Abernathy, A. E. Becerra-Toledo, H. Armandula, E. Black, K. Dooley, M. Eichenfield, C. Nwabugwu, A. Villar, D. R. M. Crooks, G. Cagnoli, J. Hough, C. R. How, I. MacLaren, P. Murray, S. Reid, S. Rowan, P. H. Sneddon, M. M. Fejer, R. Route, S. D. Penn, P. Ganau, J.-M. Mackowski, C. Michel, L. Pinard, and A. Remillieux, *Class. Quantum Grav.* **24**, 405 (2007).

¹⁸M. Paternostro, D. Vitali, S. Gigan, M. S. Kim, C. Brukner, J. Eisert, and M. Aspelmeyer, *Phys. Rev. Lett.* **99**, 250401 (2007).